CO₂ Removal via an Environmental Green Solvent, K₂CO₃−Glycine (PCGLY): Investigative Analysis of a Dynamic and Control Study

Faezah Isa, Haslinda Zabiri,* Noorlisa Harun, and Azmi M. Shariff

ACCESS | Metrics & More | Article Recommendations

ABSTRACT: Promoted potassium carbonate with glycine has been actively investigated as a chemical solvent for the removal of CO_2. Though a vast number of studies have been reported for potassium carbonate, dynamic studies regarding this promoted solvent are not yet extensively reported in the literature. In this work, a steady-state simulation has been performed via an equilibrium stage model in Aspen Plus V10 using the experimental data of an absorber from the bench scale pilot plant (MINI CHAS) located in Universiti Teknologi PETRONAS. In this study, 15 wt % K_2CO_3 + 3 wt % glycine is utilized as the medium for absorption, and the operating pressure is set at 40 bar to imitate the natural gas treatment process. The removal observed from the pilot plant is about 75% and the steady-state simulation with a tuned vaporization efficiency managed to replicate a similar result. The transient analysis is performed via activating a flow-driven method, and the simulation is transferred into Aspen Dynamic. A simple control strategy using a proportional−integral (PI) controller is installed at the gas outlet to monitor the CO_2 composition, and further disturbances are introduced at the inlet gas flow rate using a step test and ramp test. The controller is tuned using a trial-and-error method and a satisfactory response is achieved under varying changes in the inlet gas flow rate. Further investigation is carried out using the model predictive controller (MPC), in which 5000 data points are generated through pseudorandom binary sequence (PRBS) analysis for state-space model system identification. The state-space model identified as the best is then used to design the MPC controller. A disturbance rejection test on the MPC controller is conducted via changing the gas flow rate at 5% and a quick response is observed. In conclusion, both MPC and PI controllers managed to produce a good response once the disturbance was introduced within the CO_2−potassium carbonate−glycine (PCGLY) system.
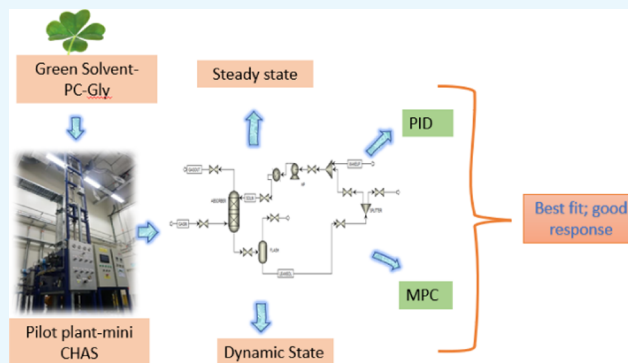
1. INTRODUCTION

The continuous exploration of new gas reserves alongside increases in global power demand necessitates the development of less demanding technologies, such that the treatment process can be accomplished at a minimized cost. One of the most common and cost-effective technologies is the chemical absorption process. This method is advantageous in its high efficiency and mature technologies as compared to other methods.[1] The cost associated with using conventional amines like monoethanolamine (MEA) and diethanolamine (DEA) are steep due to high volatility, high solvent degradation rate, and high regeneration energy requirement. The high regeneration energy that severely increases the uptake of electricity by up to 70−80% has led many global researchers to explore other potential solvents.[2]

Absorption processes based on glycine-promoted carbonate solvents are currently of interest as a technical alternative that has the potential to overcome the high regeneration energy requirement of amine-based solvents.[3−6] However, the use of the newly promoted solvent is held back by its lack of studies and

performance assessments under a wide range of conditions at a larger scale. Unlike CO_2 capture via amines, no dynamic analysis has been reported under both lab-based or scaled-up conditions for this process. Direct utilization of the new green solvent cannot be simply implemented without basic knowledge of its behavior in large-scale applications. Hence, modeling and simulations are required to observe the complex interplay between the chemical and physical properties under scale-up conditions, especially during the transient process.

Potassium carbonate (PC) is well known among CO_2 removal processes, with the addition of promoters being actively investigated.[7−9] Process optimization, energy analysis, and

economic performance have been extensively studied at the steady-state level, but this study is not sufficient in predicting the operability of the plant in the presence of continuous and sudden system fluctuations. To date, many dynamic studies and modeling are reported for the process of CO_2–MEA,[10−13] though none so far for the K_2CO_3 system, especially with glycine acting as a solvent promoter. Therefore, the novelty in this work is contributed in three aspects.

(i) The utilization of low-concentration potassium carbonate–glycine (PCGLY) for the removal of CO_2, which is mixed at the ratio of 15 wt % + 3 wt %. This is necessary to achieve the green solvent title as it has low toxicity levels and will also avoid salt precipitation, preventing the presence of acids in the solvent.[6,14] In addition to that, the high operating pressure and low concentration of the solvent were successful as the flash tank managed to recover the intended solvent without passing through a stripping column. Hence, the capital cost and operating cost can be optimized.[7,8,14]

(ii) In the open literature, the first principal model and complicated rate-based method are commonly found for the dynamic analysis during the MEA–CO_2 absorption process.[11−13] Hence, this work uses a simple equilibrium approach with a tuned vaporization efficiency in the standard simulation program of Aspen Plus/Dynamic to observe the transient behavior.

(iii) To control the process, many control strategies are proposed[13,15,16] and in this study, a basic proportional–integral (PI) feedback control strategy is installed in a closed-loop system. System identification using the pseudorandom binary sequence (PRBS) signal is conducted to generate 5000 data points and exported to the Matlab. The 2nd order state-space model is selected to produce the best fit between the measured and simulated data before the model predictive controller (MPC) can be designed.[17,18] The set point change is introduced and the response from the input–output behavior is observed.

This work is the first attempt to test the performance of a CO_2–PCGLY system in the dynamic state. Hence, the key input process variable (mainly gas flow rate in the GASIN stream) is disturbed to observe the key output responses (CO_2 mole composition in the GASOUT stream) to ensure that the desired removal is achieved throughout the process. A +5% step change, ramp, and sinusoidal tests are conducted to observe the PI controller performances. The controller response is further improved by tuning the gain and time integral. Then, the performance between the promoted solvent and unpromoted solvent in terms of the absorption rate is observed. An advanced controller such as the MPC is always desirable since a fast action controller is very essential to correct any deviations, especially in the CO_2 removal target. Therefore, the MPC model is proposed to predict the future behavior of the system. The results from the dynamic model developed for this process have the potential to provide insight regarding the continuous process at the scale-up level for the K_2CO_3–glycine–CO_2 process. Hence, it has high candidacy as a basis to further develop control strategy mechanisms related to operability.

2. RESEARCH METHODOLOGY

The workflow in this study is segregated into three different stages. Initially, all of the physical properties including the Experimental Data are obtained from the literature. Then, the

stand-alone absorber is simulated using the equilibrium stage method by varying the number of stages and column efficiency. The efficiency is tuned until the correct removal is achieved, and then the dynamic mode is activated via the flow-driven method. Once convergence is achieved, the simulation is transferred into Aspen Dynamics. A basic PI controller is evaluated including the controller tuning and comparative performance between promoted and unpromoted solvents. A part of the analysis comprises data generation using the PRBS signal for the development of system identification prior to designing the MPC controller. Further elaboration is explained under the following subsections.

2.1. Experimental Data. The main purpose of the experimental work is to collect the actual data for the purpose of validation. Hence, in this study, Experimental Data are extracted from the literature that is reported by Mustafa et al.[6] Initially, potassium carbonate and glycine with purity (99%) are prepared and well mixed based on the following ratio, (15 wt % PC + 3 wt % glycine). The bench scale pilot plant, MINI CHAS (carbon hydrogen absorption system), located in CO_2 Capture Research (CO_2RES), University Teknologi PETRONAS consists of a single absorber, high-pressure pump, compressor, and CO_2 data analyzer. The absorber column of the MINI CHAS is specifically designed to be operated at high pressures of up to 100 bar to emulate natural gas treatment plants, and two experimental runs have been successfully observed under this plant, CO_2–PCGLY[6] and CO_2–piperazine-aminomethyl propanol (PZAMP).[19] The column height is about 2.04 m with an internal diameter of 0.046 m.

In this work, countercurrent absorption occurs when the gas is compressed into the column with the flow rate maintained at 41.72 kmol/m^2 hr until the operating pressure inside the column reached 40 bar. To imitate the high CO_2 content of natural gas, a mixture of 20 mol % CO_2 and 80 mol % CH_4 is combined in a gas mixer before it is compressed to the bottom of the absorber. The initial mole fraction of CO_2 inside the column is recorded and once the value is stable, a liquid solvent is introduced at the top of the column via a high-pressure pump with a flow rate set at 0.2 L/min. The lean solvent inside the storage tank is heated up until it reaches the desired value of 60 °C. These operating conditions and column specifications are summarized in Table 1. The process flow diagram including the actual absorber of MINI CHAS is shown in Figure 1.

The physical properties of potassium carbonate–glycine are not widely available in the literature. Thus, a solubility analysis has been conducted and reported by the author to observe the efficiency of absorption of potassium carbonate with glycine at different concentrations.[20] Another reported solubility data[21] has shown that 15 wt % PC + 3 wt % glycine is sufficient for the removal of CO_2 at high pressure, thus encouraging the experimental work to be conducted at a bench scale mini pilot plant.[6] Then, regression of physical properties, particularly the density and viscosity that were obtained from the literature,[22] are carried out in Aspen Plus.

2.2. Steady-State Development and Simulations. *2.2.1. Equilibrium Stage Model.* The equilibrium method is represented by a simple set of equations, and the accuracy is highly dependent on the prediction of the Murphree or vaporization efficiency.[2] The utilization of the Murphree efficiency has long been used for simulation development and helps to correlate the theoretical stages and the actual trays in the column. This efficiency can be based upon the liquid or the vapor composition on a particular stage at certain conditions of

Table 1. Specification of the Absorber Column in a Bench Scale Pilot Plant (Mini CHAS) and Operating Conditions

parameter	operating condition
temperature of feed gas	40 °C
pressure of feed gas	40 bar
composition of feed gas	80 mol % CH_4, 20 mol % CO_2
flow rate of feed gas	41.72 kmol/m^2 h
temperature of solvent	60 °C
pressure of solvent	40 bar
composition of solvent	PC 15 wt % + Gly 3 wt %
flow rate of solvent	0.2 L/min
packing height	2.04 m
column diameter	0.046 m
cross-sectional area	1.67×10^{-3} m^2
void fraction	0.9
corrugation inclination angle	60°
corrugation side angle	8.9 mm
surface area	500 m^2/m^3
material	sulzer material gauze

temperature and pressure. In the equilibrium stage-based method, perfect mixing based on the countercurrent reaction is assumed to occur at each stage and phase equilibrium is achieved before it travels from one stage to another. However, since this is impossible to occur under realistic conditions, the efficiency concept is introduced as an effective approximation. The utilization of efficiency adjustments under the equilibrium approach to simulate the dynamic analysis has been reported in a few studies.[23,24]

Another important aspect of the equilibrium stage model is to obtain the correct equilibrium rate constant for each of the reactions. In this work, two reaction mechanisms are considered: solvent reactions and promoter reactions. Glycine might exist in three different states when diluted into an aqueous solution, which includes protonated, zwitterionic, and anionic forms. Protonated (glycinium) and zwitterionic species might appear during the process but they do not affect the reaction. A component of interest is the anionic form of glycine, or glycinate

(Gly-). Since it is basic, it will react with CO_2 in aqueous solutions to form unstable zwitterion glycinate before rapidly losing a proton to form stable carbamate.[25,26] Then, the hydrolysis process will take place between carbamate and water to form the glycinate species again. These three reaction mechanisms are shown in R8−R10.

A high concentration of potassium carbonate is not advisable as it may cause precipitation in the column or tubing, therefore the advisable concentration for the solvent must be below 30 wt %.[7] The overall reaction of potassium carbonate with CO_2 is shown in R1, and the dissociation of the solvent is assumed as in R2. The instantaneous reaction that occurred in R3 is considered as an acidic mechanism and is assumed to be negligible. The self-ionization of water takes place in R4, and the following R5 is the elementary step that serves as the rate-controlling step.[4,25,26] The reactions R6 and R7 show how CO_2 is absorbed into the water to form hydronium and hydroxide ions.[1,26] Figure 2 shows the countercurrent absorption process together with the solvent and promoter reaction in the process.

Based on the above reaction, the mathematical equations that govern the equilibrium stage model is simplified below.[2] The overall mass balance in stage n is described by eq 1, with L and V representing the liquid and gas flow rates, respectively.

$$L_{n+1} - L_n + V_n - V_{n-1} = 0 \tag{1}$$

Mass balance of the species in every stage is explained in eq 2, with x and y as the mole fractions of every species, i.

$$L_{n+1}x_{n+1,i} - L_n x_{n,i} + V_n y_{n,i} - V_{n-1}y_{n-1,i} = 0 \tag{2}$$

The energy balance of stage n is calculated via eq 3. H_G and H_L are the enthalpies of the gas and liquid, respectively, while ΔH_{CO2} is the heat of absorption of CO_2, and ΔH_{H2O} is the heat of water vaporization.

$$L_{n+1}H_{n+1}^{L} - L_n H_n^{L} + V_n H_n^{G} - V_{n-1}H_{n-1}^{G} + (\Delta H_{Co_2})_n$$
$$- (\Delta H_{H_2O})_n = 0 \tag{3}$$
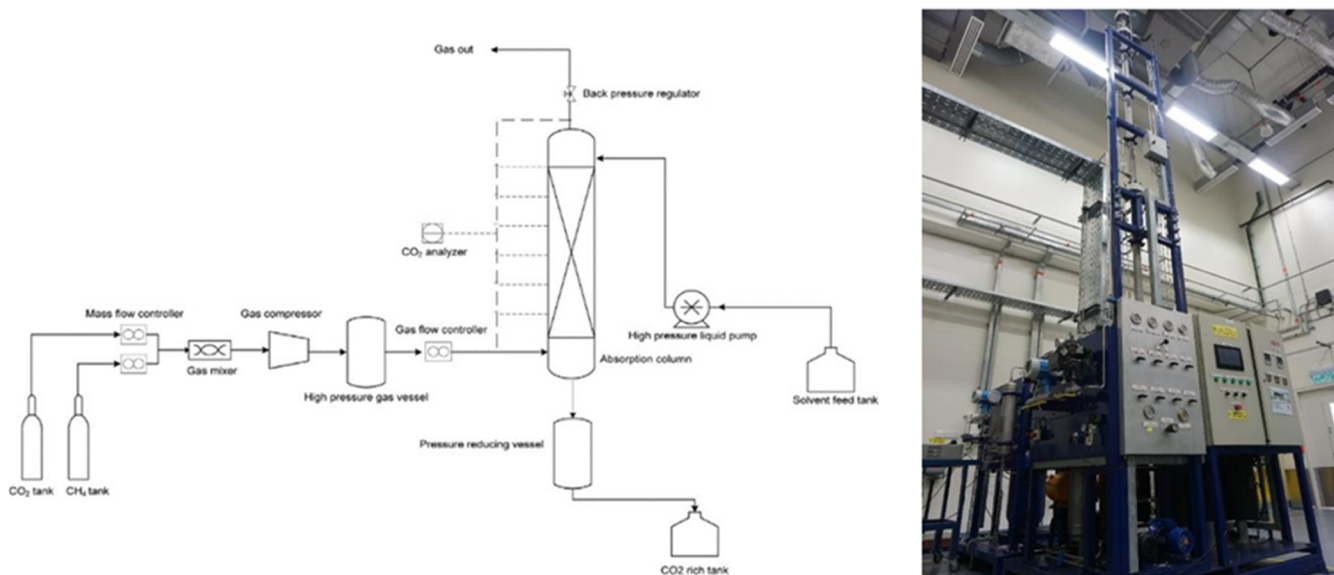
Figure 1. Process flow diagram and the structured packing absorber of the bench scale pilot plant MINI CHAS (carbon hydrogen absorption system) located in Universiti Teknologi PETRONAS.
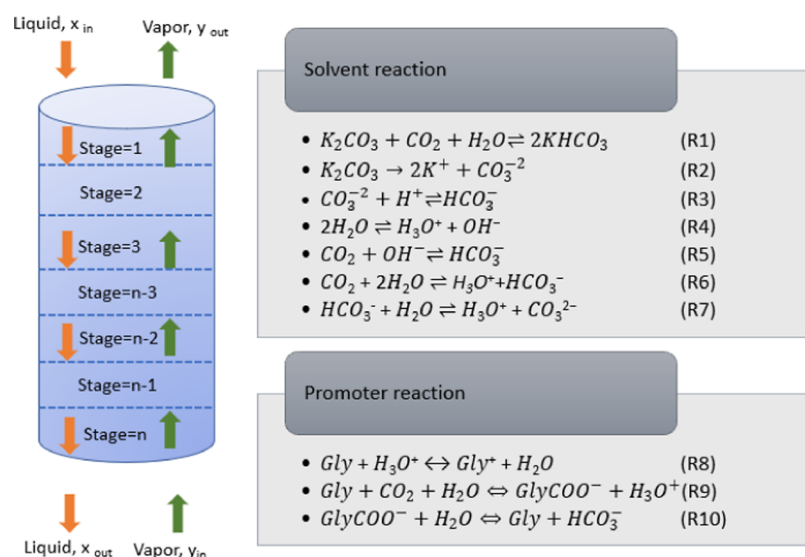
Figure 2. Countercurrent flows for the equilibrium stage model and the overall reactions.

$$r = k \exp\left(-\frac{E}{RT}\right) \prod_{i-1}^{N} c_i^{\alpha i} \tag{4}$$

The rate constant for R5 can be described using the power law kinetic as shown in eq 4, where r is described as the reaction rate, k is the pre-exponential factor, T is the temperature in Kelvin, E is the activation energy (J/mol), R is the gas constant (8.314 J/mol K), N is the number of components, C_i is the concentration of component i, and α is the exponent of component i. The values of the constants for the reaction kinetics are summarized in Table 2.[1]

Table 2. Constant Values for the Kinetic Reaction

reaction	k	E (J/mol)
$CO_2 + OH^- \rightarrow HCO_3^-$	4.32×10^{13}	55470.9
$HCO_3^-{}_2 \rightarrow CO_2 + OH^-$	2.38×10^{17}	123305.5

The equilibrium constants are described by the van't Hoff equation as shown in eq 5, and the values of the equilibrium constants are presented in Table 3. Some of the values are obtained from the literature[25] as well as from Aspen itself.

$$\ln K_i = A_i + \frac{B_i}{T} + C_i \ln T + D_i T \tag{5}$$

2.2.2. Scale-Up of Steady-State Simulations. In this study, CO_2 removal via promoted potassium carbonate with glycine has been developed in Aspen Plus V10 using the ENRTL method. This thermodynamic fluid package is selected since the system investigated is a nonideal process, and thus the activity

Table 3. Constant Values for the Equilibrium Reaction

reaction	A	B	C	D
$2H_2O \rightleftharpoons H_3O + {}^+OH^-$	132.9	−13345.9	−22.48	0
$CO_2 + 2H_2O \rightleftharpoons H_3O^+ + HCO_3$	231.46	−12092	−36.78	0
$HCO^- + 2H_2O \rightleftharpoons H_3O^+ + CO_2^-$	216.05	−12432	−35.48	−0.14
$Gly + H_3O^+ \rightleftharpoons Gly^+ + H_2O$	−516.04	20158.62	90.48	
$KHCO_3 \rightleftharpoons K^+ + HCO^-$	−274.72	9544.26	41.34	

coefficient model is preferred. In addition, it provides a wide range of estimations such as fugacity, diffusion, enthalpy, and entropy.[27,28] The utilization of the ENRTL model has been successful for many CO_2 absorption processes for various types of solvents such as MDEA,[29] AMP-PZ,[30] PZ,[31] PC,[1] etc. Since the properties of potassium carbonate and glycine such as the reaction equilibrium constant, physicochemical properties including scalar and temperature dependency, binary parameter, and electrolyte pair are available in the Aspen data bank, these data are retrieved and utilized to simulate the process.[32] Nonetheless, several other properties are also referred from the literature to improve this model and these literature studies are summarized in Table 4.

The actual bench scale MINI CHAS pilot plant consists of a single absorber tailored for CO_2 removal. Hence, the scale-up that includes a complete recycle is designed and validated with the actual steady-state result. In the Aspen Plus simulator, the absorber column is simulated using the Radfrac type of column,[35−37] and the process is conducted under the equilibrium approach. This method offers two types of efficiencies as tuning factors to improve the prediction of the column composition, which are the Murphree efficiency and vapor efficiency. Basically, once absorption takes place, the rich solvent is collected and transferred to a flash tank. The flash tank will reduce the pressure of the solution, and thus will facilitate the separation of CO_2 and CH_4 from the rich solutions. The liquid solvent is then recycled back to the top of the column using a high-pressure pump. A cooler is installed right before the solvent enters the column to ensure that the solvent temperature is maintained at the desired value. The CO_2 mole fraction is continuously observed in the GASOUT stream using a gas analyzer, as shown in Figure 3.

2.3. Dynamic Model and Simulations. Since the steady-state analysis is not sufficient for transient analysis, the dynamic mode is activated in Aspen Plus for this purpose. There are two methods to simulate the dynamic model, which are pressure driven, or flow driven. In this work, flow driven is selected as it is much easier to converge. The pressure-driven mode is preferred when the pressure of the system is significant in the gas phase. The flow-driven mode is suitable for liquid-phase systems or systems with good pressure and flow control. Conversion to

Table 4. Summary of Physiochemical Properties for Simulation Development

type of properties	concentration	temperature	pressure	reference
equilibrium constant	glycine 0.64–1.36 mol/kg	50–60 °C		Lee et al.[25]
solubility	15 wt % potassium carbonate + 3 wt % glycine	30–50 °C	2–10 bar	Shaikh et al.[21]
density	15 wt % potassium carbonate + 3 wt % glycine	25–65 °C	1 bar	Shuaib et al.[22]
viscosity	15 wt % potassium carbonate + 3 wt % glycine	25–65 °C	1 bar	Shuaib et al.[22]
vapor pressure	glycine, 0.1006–3.299 mol/kg	25 °C		Kuramochi et al.[33]
activity coefficient	glycine, 0.1006–3.299 mol/kg	25 °C		Kuramochi et al.[33]
solubility	sodium glycinate 5–25 wt %	40–60 °C	1–7 bar	Mondal et al.[34]
solubility	10.24 wt % potassium carbonate + 3 wt % glycine	100–120 °C	1–2 bar	Grimekis et al.[8]
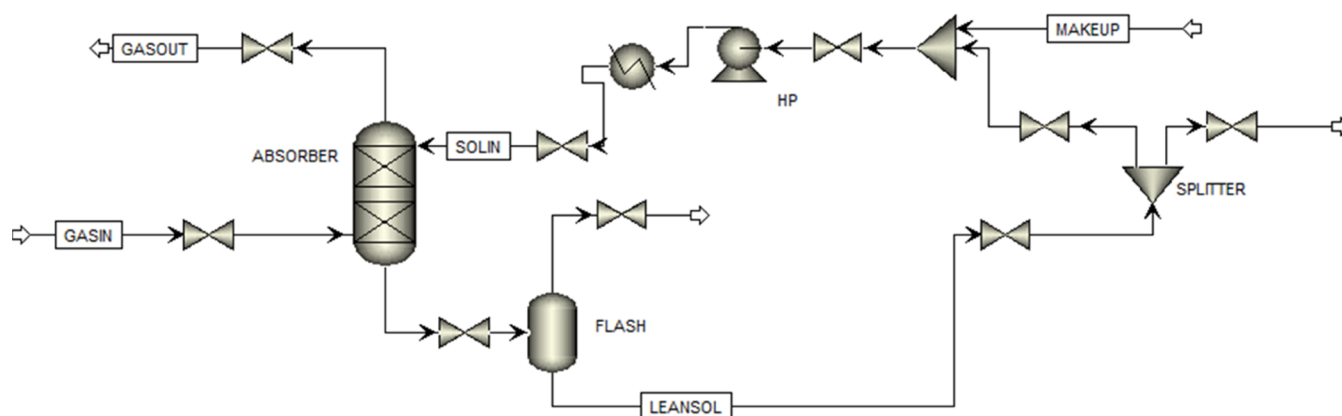
Figure 3. Steady-state simulation of CO_2–PCGLY in Aspen Plus.
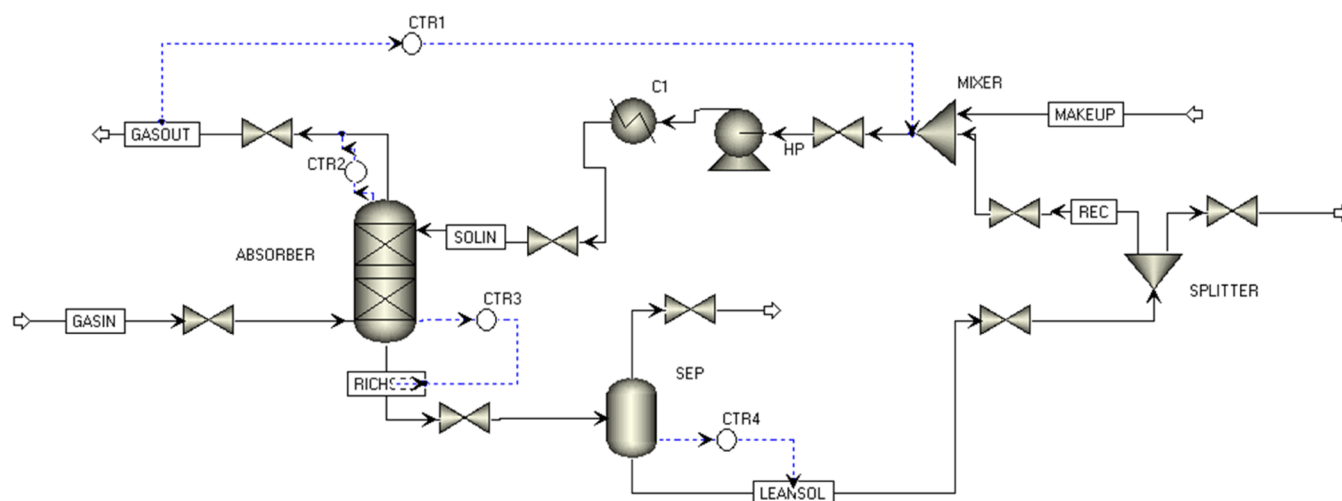
Figure 4. Dynamic simulation with the basic controller.

Aspen Dynamics requires several additional inputs that need to be specified. This includes equipment sizing and the hydraulics information for each of the equipment, including valves for every stream. Once all of the necessary information has been provided and a pressure check has been performed, the dynamic simulation is transferred into Aspen Dynamics.

Figure 4 shows the complete flowsheet for transient analysis in Aspen Dynamics. The necessity of a dynamic model is very important for the development of an effective basic regulatory control. During this study, scenario 1, which consists of an absorber, is further equipped with a basic controller to keep the controlled variables such as the flow rate and pressure within the desired set points (SP). The controllers are tuned based on the different gain (K_c), integral (τ_I), and derivative (τ_D) values to

observe the corrective action of the controllers, as shown in Table 5.

3. RESULTS AND DISCUSSION

The results of the Aspen Plus simulation are compared with the actual result from the MINI CHAS bench scale pilot plant. Since only the absorber is physically available in the MINI CHAS, the validation is focused only on the removal obtained at the sweet gas line from the top of the absorber. In the experimental run, CO_2 samples are collected from the CO_2 gas analyzer and recorded until the process achieved a steady state. Then, the removal of CO_2 is calculated from the simple formulation as shown in equation eq 6

Table 5. PI Controllers and the Tuning Values

controller	C_v	M_v	tuning values
composition controller (CTR 1)	CO_2 in GASOUT	lean solvent flow rate	$K_c = 2$ $\tau_I = 0.2$ $\tau_D = 0$
pressure controller (CTR 2)	column pressure	gas out flow rate	$K_c = 20$ $\tau_I = 12$ $\tau_D = 0$
level controller (CTR 3)	sump level	rich solvent flow rate	$K_c = 10$ $\tau_I = 60$ $\tau_D = 0$

$$CO_2 \ \text{removal}(\%) = \frac{CO_2, \text{in} - CO_2, \text{out}}{CO_2, \text{in}} \qquad (6)$$

3.1. Stage Efficiency Tuning. The separation of CO_2 using PCGLY in this work employed the Radfrac type column, and one of the main parameters needed to be provided is the number of stages. Since there is no actual tray in the column, a simple formulation as shown in equation eq 7 is used. However, the height of the equivalent theoretical plate (HETP) for this structured type packing is not available, therefore, the number of stages is treated as a tunable factor.

$$\text{no of stages} = \frac{\text{height}}{\text{HETP}} \qquad (7)$$

Since the equilibrium method is adopted in this work, the stage efficiency is also considered as a tunable factor to improve model accuracy. There are two types of stage efficiency in Aspen Plus: vaporization efficiency and Murphy efficiency, which can be entered either for components, stages, or columns. The vaporization efficiency and Murphree efficiency are described in equations eqs 8 and 9. The liquid and vapor mole fractions are presented as y and x, respectively, K is the equilibrium constant, while i and j are the components and number of stages, respectively.

$$\text{effiency}_{\text{vaporization}} = \frac{y_{ij}}{K_{ij}x_{ij}} \qquad (8)$$

$$\text{effiency}_{\text{Murphree}} = \frac{y_{ij} - y_{ij+1}}{K_{ij}x_{ij} - y_{ij+1}} \qquad (9)$$

Table 6 shows the manipulated stage efficiency using the vaporization type efficiency. The number of stages is maintained at 7 as it gives the best removal as the actual process. This is also prior to the sampling point of the column itself as shown by Hairul et al.[39] As observed in Table 7, the highest removal is

obtained when the stage efficiency at the bottom of the column is specified at 0.09. This indicates that the vapor entering the column has reduced saturation since the efficiency will change the equilibrium constant of the vapor–liquid equilibrium. The efficiency will alter the volatilities of the components, which are calculated by the property model. However, using 0.09 results in overestimation of the CO_2 removal beyond 75% of the actual Experimental Data. Hence, the stage efficiency is further tuned between 0.09 and 0.1 to give a more accurate removal, from which the final optimum value is achieved when the efficiency is specified at 0.092. The utilization of efficiency for simulation improvement has also been conducted by Smith et al.[40] where the Murphree efficiency is adjusted between 0.024 and 0.15 to match the capture rate between the pilot plant and simulation. A capture rate of CO_2 between 3.8 and 40% is obtained in this study with the solvent concentration varying from 30 to 45 wt %.

Further analysis is conducted for the Murphree efficiency tuning, and the results are presented in Table 7. A similar method is applied as the vaporization efficiency where the tuning is introduced at the bottom stage where the gas enters the absorption column. However, the removal obtained by manipulating the Murphree efficiency has minimal impact on the CO_2 removal. There are no significant changes in the column CO_2 composition profile as the values are tuned from 0.9 to 0.1. Referring to the formulae of vaporization and Murphree efficiency eqs 8 and 9, it seems that vaporization efficiency has a greater impact on the equilibrium constant, thus a small alteration to the efficiency has a higher impact on the overall VLE calculation for the phase equilibrium. Thus, the Murphree efficiency is ignored, and the equilibrium stage method with the vaporization efficiency at 0.092 is used as a base case for further analysis at a steady state before dynamic analysis can be commenced.

3.2. Absorber Profile. Figures 5 and 6 show the absorber profile in terms of temperature and CO_2 mole fractions along with the column height. In Figure 5, the temperature inside the column is increased slightly as the solvent moved toward the bottom (stage 7) of the column. This indicates that absorption vigorously occurs at the lower stage of the column before it exits to the rich solvent stream. Similar findings are also reported by Ochieng et al.[38] but the process has adopted hot potassium carbonate for the absorption, and thus the temperature difference is more significant. The bulge that is observed in Figure 5 indicates that the reactive and forward reactions are favored in this region.[19] The inlet solvent temperature is set as 60 °C since the high solvent temperature will resultantly contribute to the CO_2 diffusion coefficient increment, and thus mass transfer performance is improved. Nevertheless, the temperature change inside the column is very mild since the

Table 6. CO_2 Removal via Tuning the Vaporization Efficiency

efficiency	0.9	0.8	0.6	0.4	0.2	0.1	0.09	0.092
stage	mol CO_2	mol CO_2	mol CO_2	mol CO_2	mol CO_2	mol CO_2	mol CO_2	mol CO_2
1	0.1892	0.1884	0.1816	0.1724	0.1411	0.0633	0.0463	0.0498
2	0.1982	0.1982	0.1973	0.1951	0.1806	0.1059	0.0825	0.0876
3	0.1987	0.1988	0.1989	0.1986	0.1933	0.1377	0.1140	0.1194
4	0.1988	0.1989	0.1991	0.1992	0.1974	0.1606	0.1402	0.1450
5	0.1988	0.1989	0.1991	0.1993	0.1988	0.1765	0.1611	0.1649
6	0.1989	0.1990	0.1992	0.1994	0.1993	0.1874	0.1776	0.1801
7	0.1989	0.1990	0.1992	0.1994	0.1996	0.1948	0.1902	0.1914
removal (%)	5.3820	5.7890	9.1895	13.7930	29.4445	68.3665	76.8701	75.1007

Table 7. CO_2 Removal via Tuning the Murphree Efficiency

efficiency	1	0.8	0.6	0.4	0.2	0.1
stage	mol CO_2	mol CO_2	mol CO_2	mol CO_2	mol CO_2	mol CO_2
1	0.189043	0.189043	0.189045	0.189079	0.189299	0.189616
2	0.19812	0.198	0.197813	0.197506	0.196844	0.195815
3	0.198626	0.198612	0.198596	0.198607	0.198597	0.19813
4	0.198675	0.198676	0.198705	0.198825	0.199086	0.199039
5	0.1987	0.198712	0.198784	0.198972	0.199315	0.199443
6	0.198725	0.198779	0.19893	0.199175	0.199512	0.199671
7	0.198765	0.199007	0.19925	0.199492	0.199734	0.199842
removal (%)	5.479	5.479	5.478	5.461	5.351	5.192
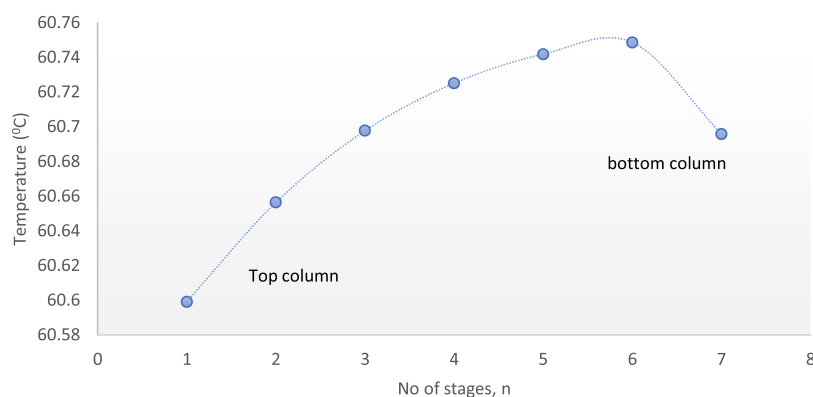
Figure 5. Temperature profile along the absorber column.
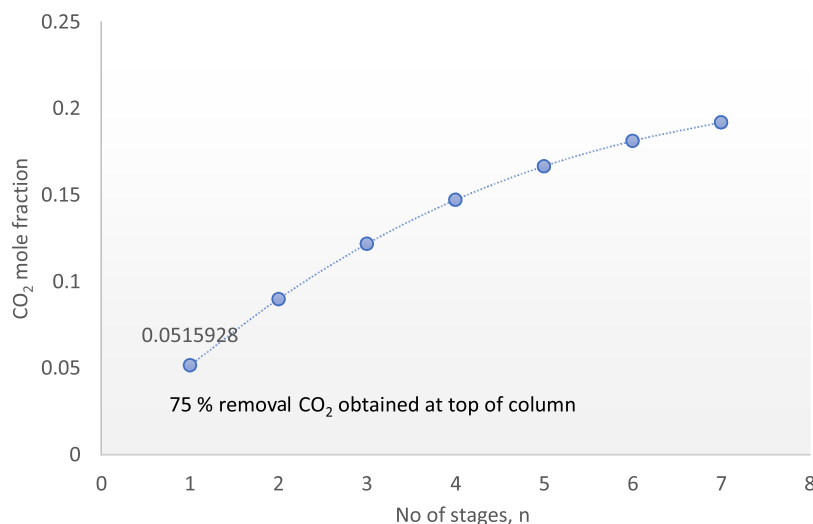
Figure 6. CO_2 profile along with the column height.

feed gas flow rate into the column is set at the minimum rate to optimize the absorption process. Based on the Arrhenius expression, the higher temperature also promotes a higher reaction rate due to the increase of k_{OH} and $k_{glycine}$.[6] According to Henry's law principle, CO_2 solubility is reduced as the temperature is increased but in this simulation, the high operating pressure and the increase of reaction constant suppressed the effect of Henry's law.[41]

The CO_2 mole fraction along the column is presented in Figure 6. The removal of CO_2 is highly dependent on the liquid to gas ratio (L/G). Theoretically, with a higher solvent rate, better removal is achieved. A high concentration of CO_2 at stage 7 is observed due to the inlet of the feed gas, which is located at the bottom of the column, and as it moved to the upper level, the

mole of CO_2 is reduced. The obtained removal in the simulation is 75.6% while the actual Experimental Data obtained is 75%, making the deviation between the experiment and the model 0.01%. From the validated removal values, the process simulation is further expanded by adding the stripper section. The removal recovery in this work is also compared with the pilot plant results from the work of Smith et al.,[4] which also utilized potassium carbonate promoted glycine as the medium for separation. The highest removal obtained in ref 4 is between 23 and 30%, with the L/G ratio varied between 3 and 5. However, their process is focused on atmospheric pressure conditions, which are specifically designed for a postcombustion process. In this study, however, the CO_2 removal process is for the treatment of natural gas, which is operated at elevated
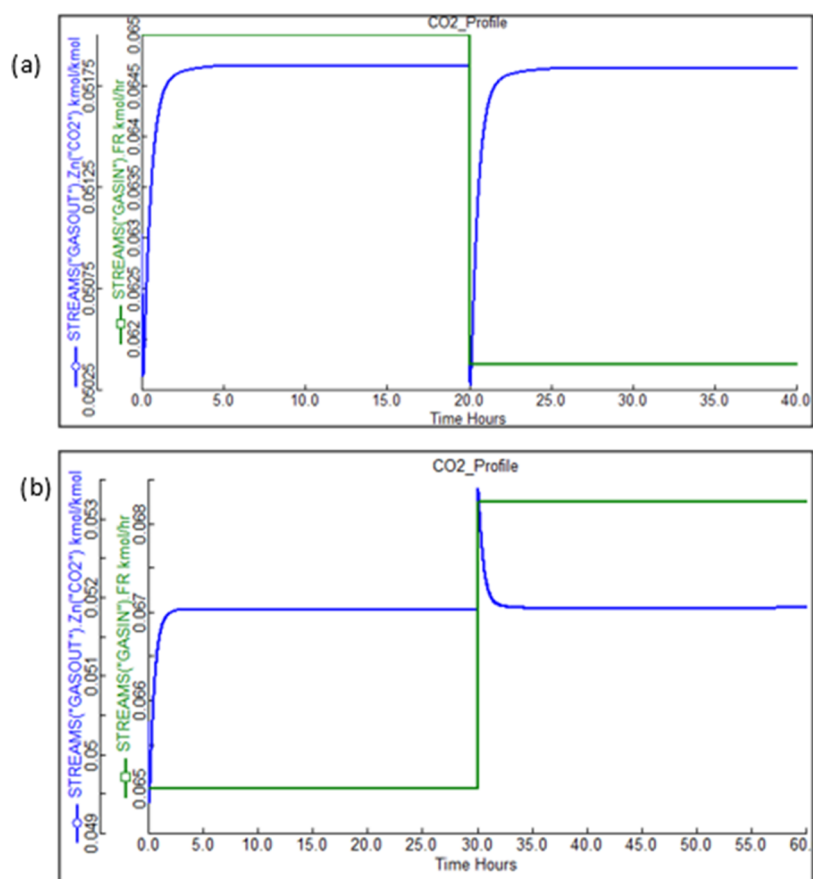
Figure 7. (a) +5 step-up change to the GASIN flow rate and (b) −5% step down of the GASIN stream flow rate.
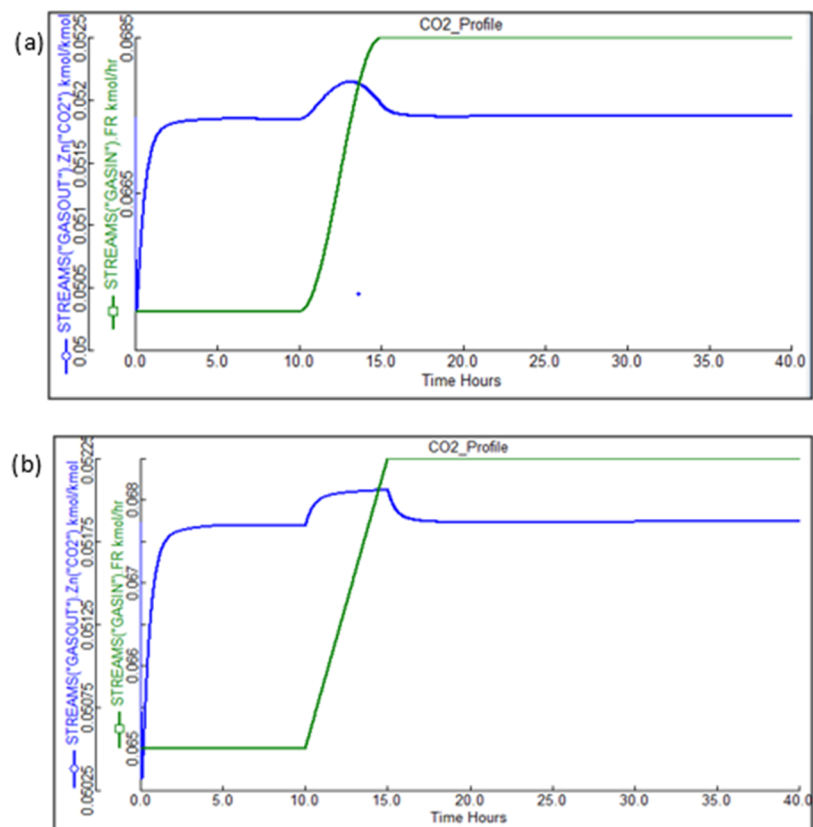
Figure 8. (a) +5% ramp test at the GASIN flow rate and (b) +5% sinusoidal test at the GASIN flow rate.
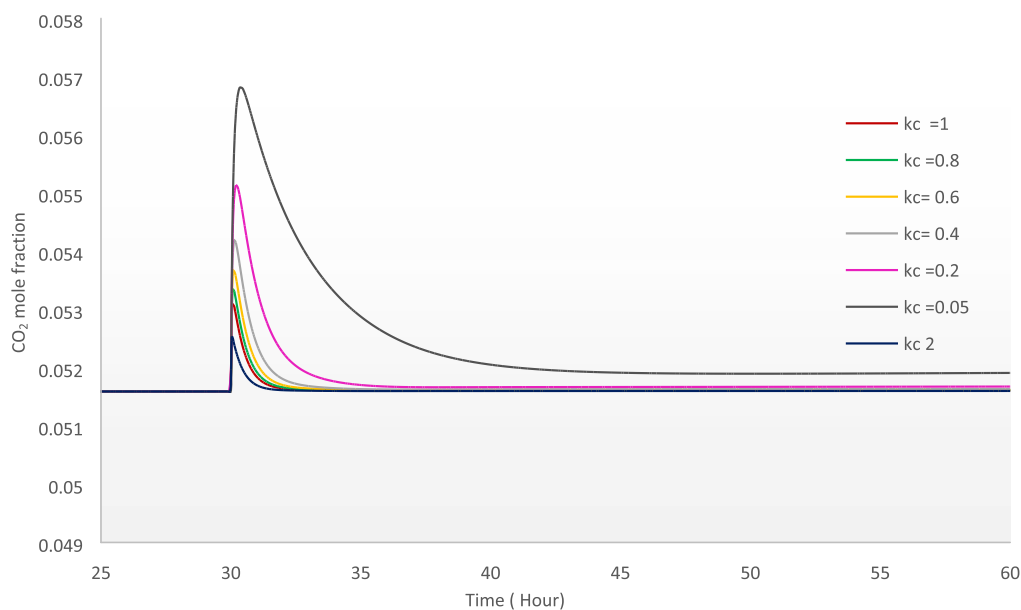
Figure 9. CO_2 profile based on the tuning of the controller gain, K_c.
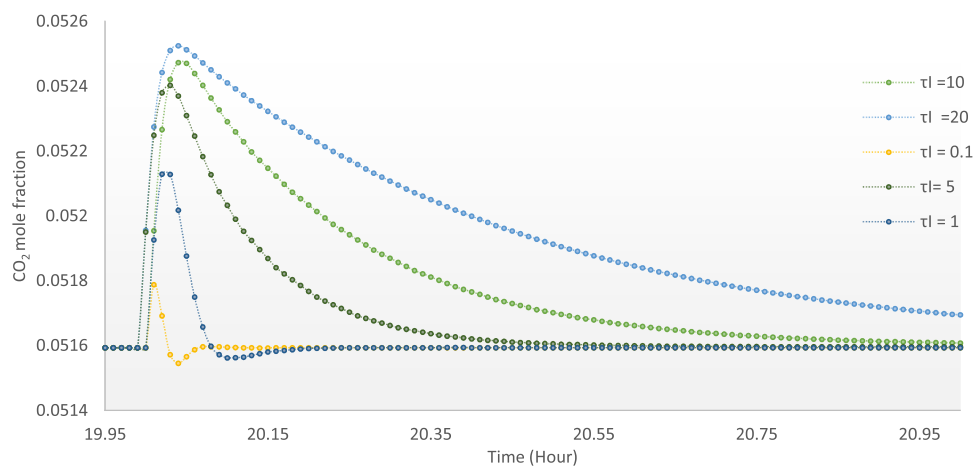
Figure 10. CO_2 profile based on the tuning of the time integral, τ_I.
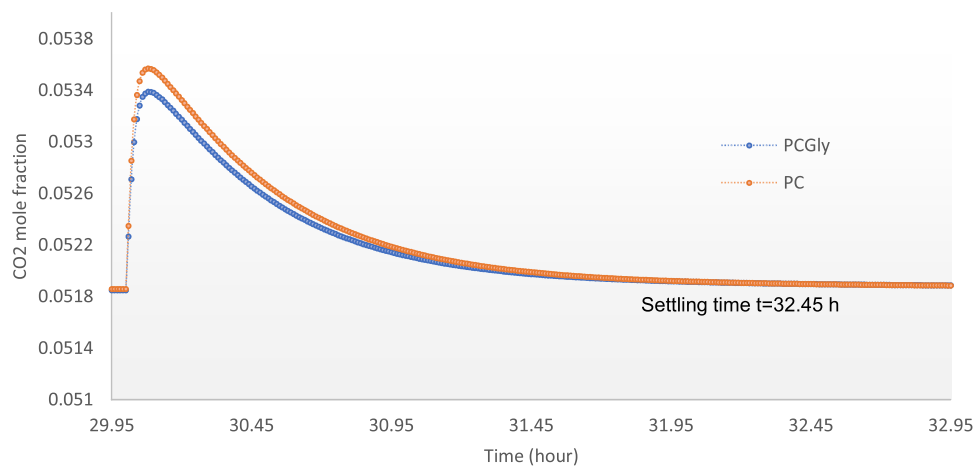
Figure 11. CO_2 mole fraction between PC and PCGLY with the default tuning value, $K_c = 1$ and $\tau_I = 20$.

pressures. As an aside, the solvent concentration is maintained as low as possible to ensure that the goal for the environmental green solvent is achieved.

3.3. Dynamic Analysis and Control Strategy. Although valuable insight can be obtained from the converged steady-state model, it is not sufficient for observing the operability of the
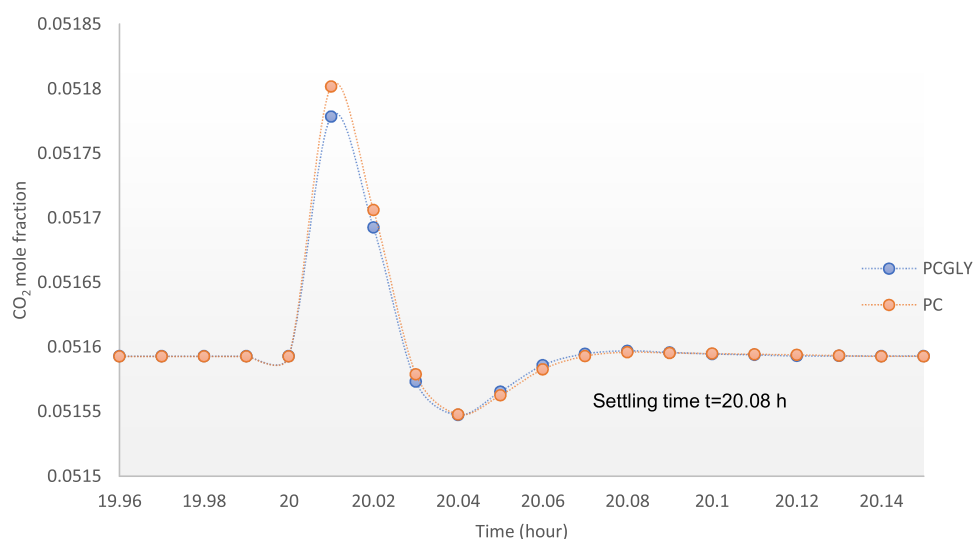
Figure 12. CO_2 mole fraction between PC and PCGLY after tuning $K_c = 2$ and $\tau_I = 0.2$.

entire pilot plant during continuous operation. Hence, the dynamic mode is activated and the model is transferred to the Aspen Dynamic for further transient analysis. Since there is no available pilot plant data for CO_2 removal via potassium carbonate with glycine during the transient process, a stand-alone absorber of the MINI CHAS pilot plant is used for validation purposes. Generally, the dynamic test can be operated in three different situations;[13]

- Ramp change in feed gas conditions.
- Step change in feed gas conditions.
- Sinusoidal change in feed gas conditions.

In this work, since the amount of CO_2 absorbed into the solvent is a key variable that needs to be controlled, a composition controller is installed at the outlet GASOUT stream, and CO_2 composition is treated as the process variable. This process variable is controlled by regulating the lean solvent flow rate. During the process, a controller will maintain the CO_2 mole fraction at the set point. When the controller detects that its value has deviated from the original set point, the valve in the lean solvent stream will be regulated until the process is returned to the set point. The increase of CO_2 gas in the sweet gas line (GASOUT stream) will force the solvent flow rate to be increased, i.e., the controller operates by directly acting as the control. In this work, the gain (K_c) value is varied from 0.1 to 2, and the integral time is maintained at the default value. After numerous trial-and-error, the optimum gain is obtained at 1, where quick corrective action is observed when a small change disturbs the gas flow rate.

3.3.1. Step Change. Within realistic natural gas processing scenarios, the flow rate of feed gas might not be constant due to leakage or maintenance. Therefore, a scenario of +5% step change is imposed on the GASIN flow rate, and the CO_2 concentration at the GASOUT stream is recorded as shown in Figure 7a. As observed, when the flow rate is increased from 0.065 to 0.06825 kmol/h (green line), the mole concentration of CO_2 (blue line) increases as well. The sudden spike of the CO_2 mole concentration is due to the lack of solvent, thus reducing the amount of CO_2 removed. However, due to the PI feedback controller action, it manages to bring back the CO_2 mole fraction to return to the original set point and once again achieve a steady state. This is to ensure that the desired removal of CO_2 is maintained at 75% during the entire process as the actual pilot

plant result. The opposite behavior is observed when a −5% step down (0.065 to 0.06175 kmol/h) is introduced into the system, as depicted in Figure 7b. When the gas flow rate is reduced, the mole fraction is instantaneously lowered, but the controller action has also cut down the solvent flow rate, thus returning the value to the original set point.

3.3.2. Ramp Test and Sinusoidal Test. The ramp and sinusoidal changes in the GASIN flow rate are also considered in this study, with a +5% increment to the initial steady-state value. As illustrated in Figure 8a, once the steady-state value is achieved after 10 h of operation, the flow rate of GASIN is slowly increased from 0.065 to 0.0685 kmol/h within 5 h of operation. As observed, the mole fraction of CO_2 that has been set at 0.051 suddenly increases and becomes unstable between 10 and 15 h. Then, once the flow rate of the GASIN stream settles at a new flow rate, the mole fraction of CO_2 in the GASOUT stream is steadily reduced to the original set point, which took about 2 h. The result obtained in this analysis corresponds to the loading of the CO_2/solvent. Whenever the mole of CO_2 increases while the mole-free carbonate is limited, a rise in CO_2 molar count will be observed in the GASOUT stream. However, a proper composition controller installed at the top of the absorber will significantly facilitate the whole operation to ensure that the removal is maintained at the desired value. A sinusoidal test in the GASIN flow rate is presented in Figure 8b. A smooth change in the GASIN flow rate caused the mole fraction of CO_2 in the GASOUT stream to fluctuate but slowly return to the original set point once the new steady state is achieved.

3.4. Effect of Gain and Integral Time Tuning. In this dynamic model simulation, a PI controller is applied as it is the most widely used in the industry for its simplicity and robust structure. The analysis is focused on the composition controller installed at the top of the column, which is used to monitor the CO_2 mole fraction in the GASOUT stream. Most tuning methods are known to be done via open-loop experimentation; however, this is time-consuming and expensive. Additionally, as a limitation of the MINI CHAS pilot plant itself, the controller requires to be conceptualized and designed via Aspen Dynamics. Hence, to modify the tuning value of the controller, it is important to identify the action of the controller. If the measured variable and manipulated variable have an inverse relationship, the reverse action is selected; and when both variables change in
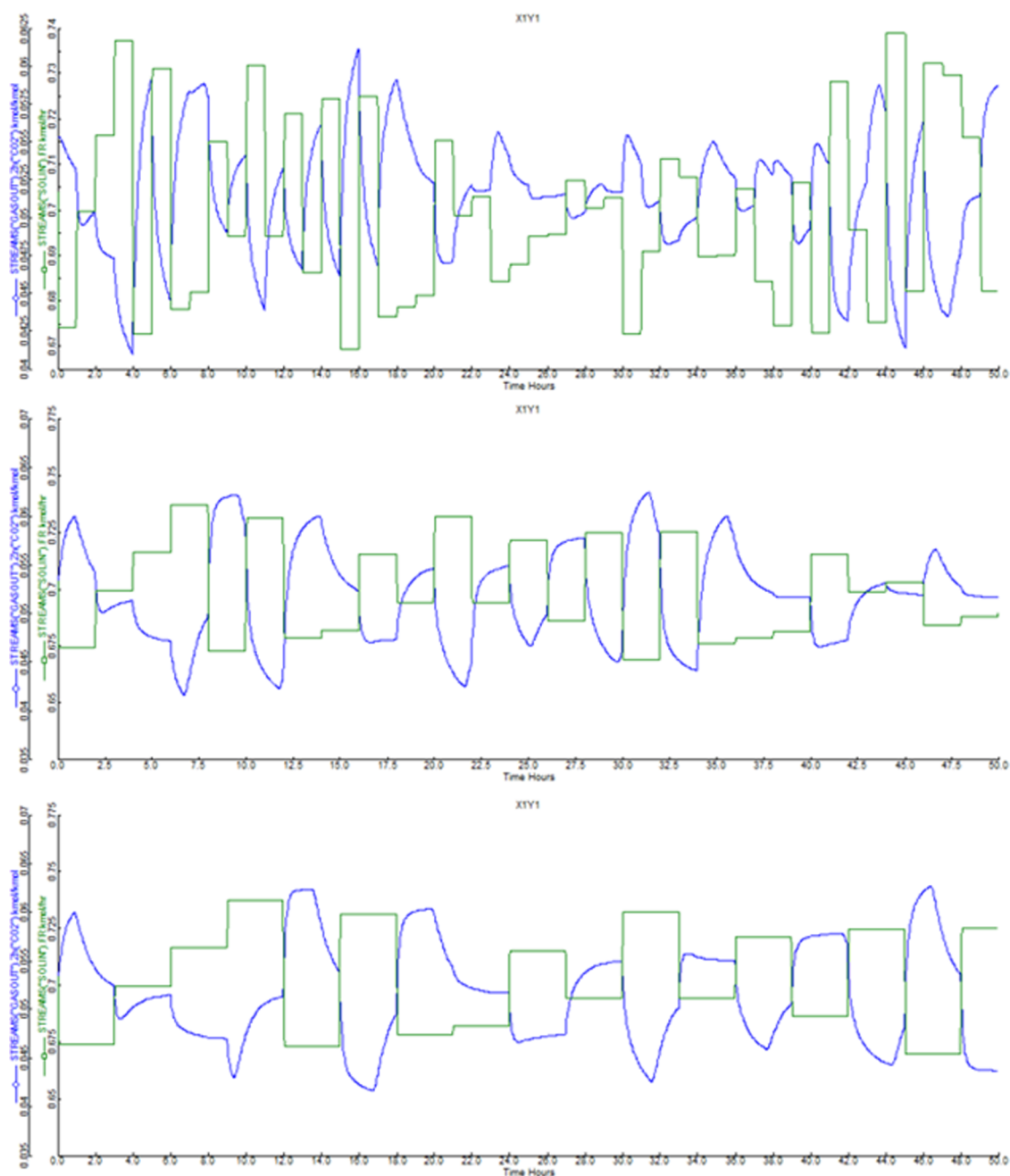
Figure 13. PRBS Signals for the input and output when the operation analysis is varied (a) 60 min, (b) 120 min, and (c) 180 min.

parallel, direct action is chosen. Normally, Aspen Dynamics will provide default values for the controller gain (K_c), integral time (τ_I), and derivative time (τ_D). Automatically initialized values are provided for the process set point, process variable range, and controller output range.

In this work, the K_c value is slowly tuned between 0.05 and 2 while the integral time is maintained at the default value, $\tau_I = 20$. Then, the mole fraction of CO_2 versus time in the GASOUT stream is plotted. A step-up change of 5% is introduced at the 30 h mark, and the settlement time of CO_2 is continuously monitored. It was observed that the lowest overshoot and shortest settling time is obtained when the value K_c is set at the maximum, the results of which are depicted in Figure 9. The settling time for the CO_2 mole fraction to achieve the set point is about 3 h, while the shortest settling time observed is at $K_c = 2$

which is about 1.5 h. With K_c maintained at a value of 2, the time integral is then tuned. In Figure 10, the time integral value, τ_I, varies between 0.1 and 20 and the shortest settling time obtained is at $\tau_I = 0.1$, which is represented by the green line. During the analysis, the process is continuously observed and once a constant value of the set point is seen, a +5% step up is introduced at the GASIN stream with a running time of 20 h. A huge deviation is produced when $\tau_I = 20$, and a longer time is needed before the CO_2 mole fraction can reach the set point. However, when $\tau_I = 0.1$, a small fluctuation is observed and the CO_2 mole fraction manages to achieve the set point at less than 0.1 h.

3.5. Comparative Analysis between PC and PCGLY. The addition of a promoter into potassium carbonate is for improving the reaction rate of absorption, enhancing its yield
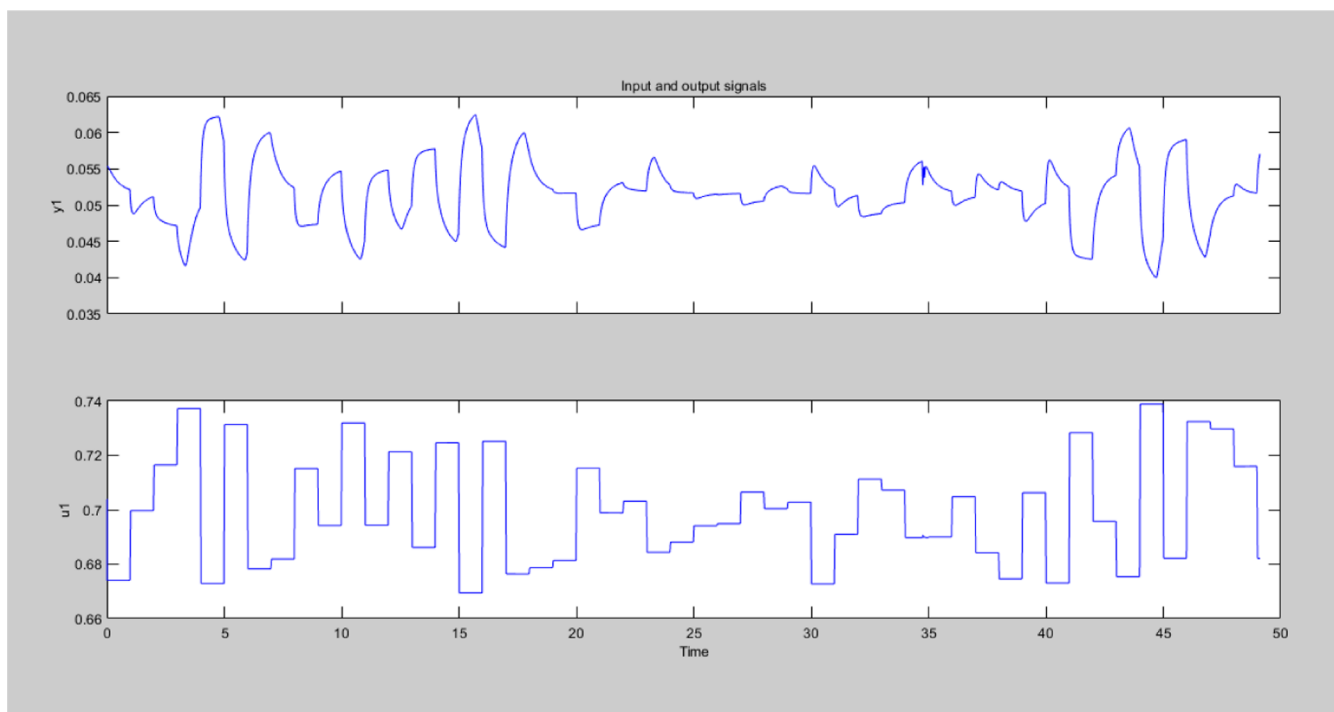
Figure 14. System identification result for the input (u_1) and output (y_1).

and performance in CO_2 removal. Hence, this comparative analysis is to observe the performance of both promoted PC with glycine and unpromoted PC from the perspective of dynamic behavior. In the steady-state simulation, 75% removal of CO_2 is obtained after tuning of the packing efficiency is done for the Radfrac absorber column. This result is successfully validated from the MINI CHAS pilot plant with a solvent concentration prepared at 15 wt % PC + 3 wt % glycine. However, the removal from unpromoted potassium is unavailable, thus a simulation is conducted using similar tuning values with a PC concentration at 18 wt %. The removal obtained from unpromoted PC is about 70% which is less compared to PC promoted with glycine.

Both systems are further equipped with additional items such as valves before they can be transported into Aspen Dynamics. The results in Figure 11 depict a profile of the CO_2 mole fraction after installation of the controller using the default values. It is observed that PCGLY has lower overshoot and higher steepness, showing that PCGLY has a better reaction rate, though the settling time between both solutions is roughly the same, which is about 2 h. Figure 12 is the result of further tuning the CO_2 composition controller for both systems, in which a similar trend can be observed. However, the slight difference is that the overshoot for the CO_2 mole composition is much lower for PCGLY than for PC. Notably, the settling time for both systems improved greatly once the controller tuning is set correctly, which is recorded at under 0.1 h. The resemblances between the two systems in performance are probably due to the use of very low concentrations of the solvent for both systems. Additionally, the concentration of glycine used is very small, which is 3 wt %, and thus the impact of the promoter on the overall system is very light.

3.6. PRBS Input Signal Design. System identification used the input and output signals of a system to identify the effectiveness of the control system for a particular process. In Aspen Dynamics, pseudorandom binary sequence (PRBS)

analysis can be carried out to test how well the system is able to reject noise. Basically, PRBS will generate positive and negative changes within the input sequence,[42] and the output will be used either as the signal itself or the noise source added into the signal. In this analysis, the open-loop system identification requires excitation signals to be imposed onto the process input, and the corresponding change in the output is then observed. Therefore, the output in the GASOUT stream (CO_2 mole fraction) is observed continuously while the input GASIN flow rate is excited with a varying amplitude of 5% from the datum value. The excitation signals are depicted in Figure 13a–c, and 5000 data points were generated from Aspen Dynamics. In Figure 13a, the period for excitation of the solvent flow rate is 60 min, followed by 120 min in Figure 13b, and 180 min in Figure 13c. The green line represents the changes in the solvent flow rate and the blue line is the response of the CO_2 mole fraction. Based on the observation, reduction of the solvent will cause the CO_2 mole fraction to increase; and when the solvent is increased, the mole fraction in the gas outlet stream will reduce. This inverse relation is true for all three PRBS analyses, in which a similar behavior is seen within the 40 h of testing. It is also noted that 3 h is still not sufficient for the process to achieve the set point, and this is reflected in the behavior, as obtained in Figure 9. With the data generated, the next strategy is to predict and interpret the behavior using the MPC.

3.7. System Identification Analysis and the MPC Designer. MPC is a process control algorithm that uses an explicit plant model and an optimizer to anticipate the desired trajectories of future output conversions from the dynamic to the steady-state model. Though PID is ubiquitous in industrial applications due to its ease of use, the MPC can be considered a more advanced option due to its predictive functionality.[42] In the MPC, a model is used to forecast the future behavior (outputs) of the system. The MPC makes predictions about the future outputs of a plant based on a dynamic model of the plant
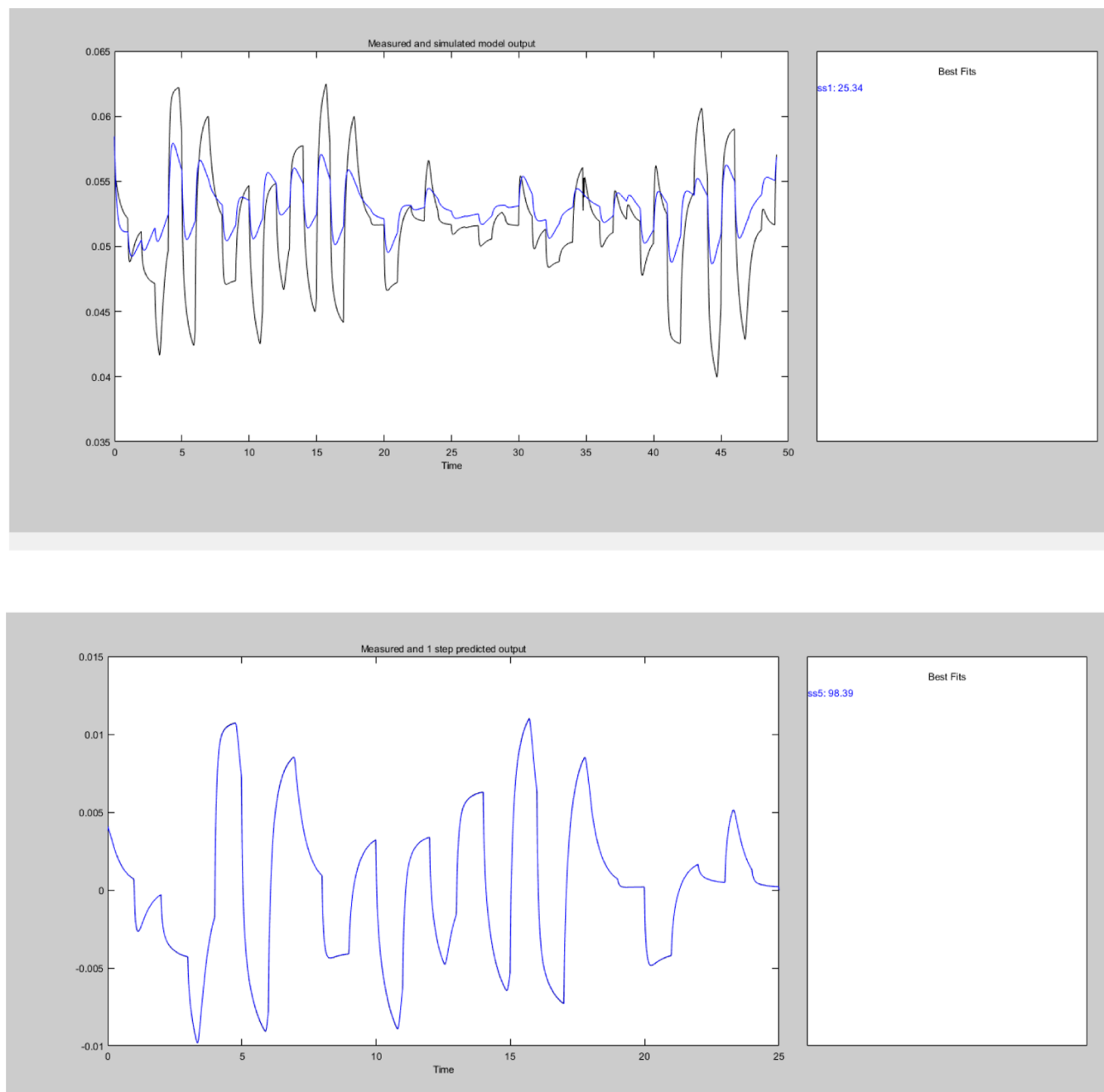
Figure 15. Simulated and measured output using the 2nd order state-space model (a) before adjustment and (b) after adjustment.

and the currently analyzed data. The objective of a controller in any control problem is to determine the most appropriate corrective action so that the output/controlled variables of the plant will be course-corrected to the desired reference/set point.[17] The implementation of an MPC structure is very limited in the CO_2 capture process, though a few studies focused on the CO_2 removal and reboiler duty aspect have been reported.[43−45]

Data generated from the previous step is first exported into Matlab, normalized between 0 and 1, and preprocessed by removing the means. The transformed continuous input−output data set is presented in Figure 14. y_1 is the process output, which represents the CO_2 mole fraction, while u_1 is the process input, which refers to the solvent flow rate. Various models are provided within the Matlab System Identification Toolbox; such as the transfer function model, state-space model, and polynomial model. The availability of these models will give the opportunity for the user to select the model that best suits the system.

In this study, the best fit between the measured and simulated data is produced when the second-order state-space model is selected. Initially, the best-fit percentage achieved is 25.34% (Figure 15a). The process model is then further improved using prediction error minimization as the estimation method while the iteration method used is the trust-region reflective method. A new best fit obtained after a few adjustments is 98.39% (Figure 15b). Thus, the best fit percentage is favorable for use in an MPC control strategy.

Implementation of the MPC is conducted using the MPC Designer. Initially, the structure of the MPC is designed by importing the data from previously identified systems. Within
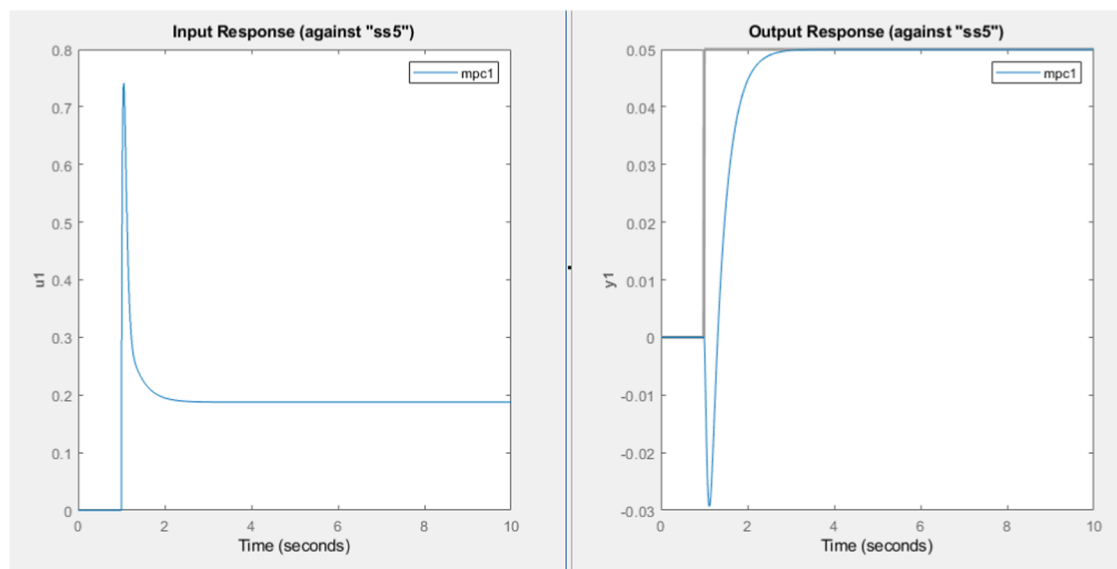
Figure 16. Input−output results of the MPC controller.
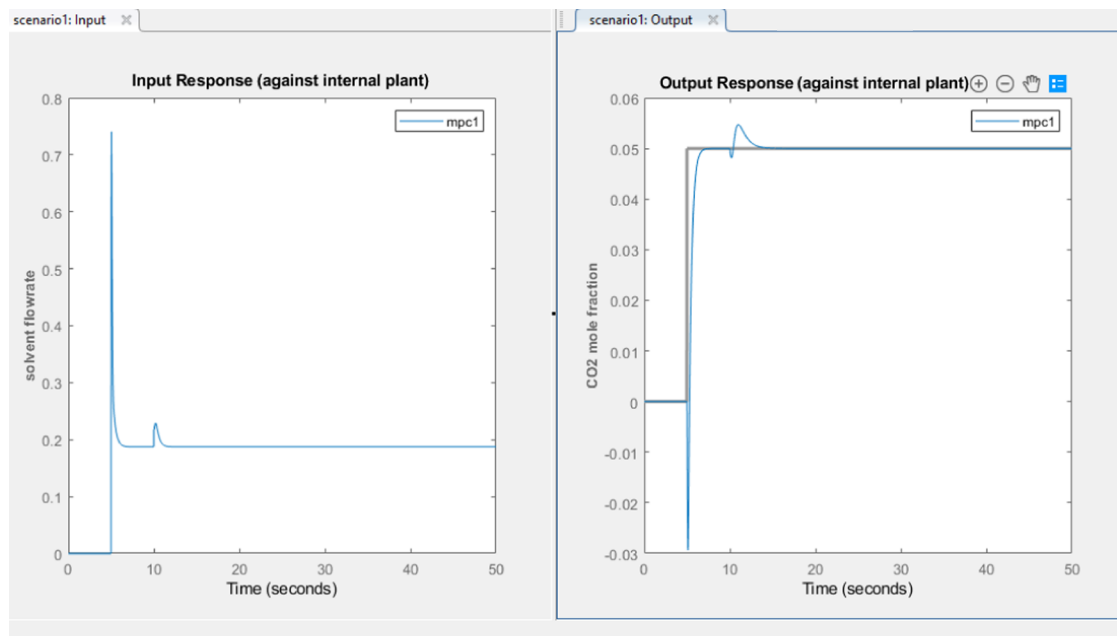
Figure 17. Successful disturbance rejection by the MPC controller.

the MPC designer, input and output responses are displayed based on the step change due to the default setting. Hence, to achieve a better result, tuning plays an important role in controller implementation. The appropriate robustness parameters, including the upper and lower bounds of the system, must be tuned by the trial-and-error method. Figure 16 shows the MPC result when the set point for the output (CO_2 mole fraction) is moved from 0 to 0.05 to achieve 75% CO_2 removal in a MINI CHAS pilot plant. In this analysis, the simulation time is set at 50 s and once the processing time reaches 5 s, the step up for the output is changed to 0.05. A corresponding response is observed in the input (solvent flow rate) where a sharp overshoot is produced before it stabilized at the value of 0.2.

The following analysis in Figure 17 shows how the MPC designer manages to reject a disturbance introduced into the system. Once the CO_2 mole fraction managed to reach the set point at 5 s, the +5% step up in the solvent flow rate is introduced at the operating time of 10 s. It is observed that a small fluctuation occurred in the CO_2 mole fraction but managed to return at the set point of 0.05. This shows that the MPC controller is able to successfully reject the disturbances introduced into the system.

4. CONCLUSIONS

A dynamic model of potassium carbonate with glycine for the removal of CO_2 to imitate the natural gas treatment has been successfully simulated using the equilibrium approach in Aspen Dynamics. The proposed model is validated using the actual steady-state bench scale MINI CHAS pilot plant operated at an elevated pressure of 40 bar with a minimum solvent concentration of 15 wt % K_2CO_3 + 3 wt % glycine. A 75% removal is achieved in the actual process, and a simulation with

tuned vaporization efficiency managed to produce a similar result. The convergence of the steady state is further analyzed in transient behavior through dynamic analysis, using the flow-driven method before transferring the model into Aspen Dynamics. A simple PI controller is installed into the system and a ±5% step test, ramp, and sinusoidal change are conducted to observe the controller performance. Further tuning for the controller gain (K_c) and integral time (τ_I) are carried out to obtain the best response in the CO_2 mole fraction in the GASOUT stream. Then, a comparative analysis between the PCGLY and unpromoted PC system focusing on the CO_2 mole fraction profile shows a similar trend, though the PCGLY system shows a better reaction rate as the steepness of the CO_2 profile is higher compared to unpromoted PC. Next, 5000 data are generated through PRBS analysis for system identification investigation. The input−output data undergo preprocessing, before the best fit between the measured and simulated is achieved. The second-order state-space model analysis produces the best fit of 98%, and thus the system is used to design the MPC structure for the process. The results from the MPC analysis show that the input and output data correspond very well to the set point changes, revealing that the CO_2−PCGLY system can be very well controlled either using an advanced MPC or a simple PID controller. Hence, a future study may be carried out to investigate the new MPC strategy for the absorber at a larger scale under a more complicated dynamic system.

AUTHOR INFORMATION

Corresponding Author

Haslinda Zabiri − *CO_2 Research center (CO2RES), Universiti Teknologi PETRONAS, Seri Iskandar 32610, Malaysia;* orcid.org/0000-0003-1821-1028; Email: haslindazabiri@utp.edu.my

Authors

Faezah Isa − *CO_2 Research center (CO2RES), Universiti Teknologi PETRONAS, Seri Iskandar 32610, Malaysia*

Noorlisa Harun − *Faculty of Chemical and Natural Resources Engineering, Universiti Malaysia Pahang, Kuantan 26300, Malaysia*

Azmi M. Shariff − *CO_2 Research center (CO2RES), Universiti Teknologi PETRONAS, Seri Iskandar 32610, Malaysia;* orcid.org/0000-0001-8524-1994

Complete contact information is available at:
https://pubs.acs.org/10.1021/acsomega.1c06254

ACKNOWLEDGMENTS

NOMENCLATURE

L, V	liquid and gas flow rates
H_G, H_L	enthalpy of the gas and liquid
ΔH_{CO2}	heat of absorption of CO_2
ΔH_{H2O}	heat of water vaporization
r	reaction rate
k	pre-exponential factor
T	temperature (kelvin)
E	activation energy (J/mol)
R	gas constant (8.314 J/mol K),
i	component

GREEK LETTERS

K_c	controller gain
τ_I	time integral
τ_D	time integral

ABBREVIATIONS

PC	potassium carbonate
PCGLY	potassium carbonate−glycine
PZAMP	piperazine−amino methyl propanol
MEA	monoethanolamine
DEA	diethanolamine
PRBS	pseudorandom binary sequence
CHAS	carbon−hydrogen absorption system
PID	proportional integral derivative
MPC	model predictive controller
ENRTL	electrolyte nonrandom two liquid

REFERENCES

(1) Li, S.; Jin, H.; Mumford, K. A.; Smith, K.; Stevens, G. IGCC precombustion CO2 capture using K2CO3 solvent and utilizing the intercooling heat recovered from CO2 compressors for CO2 regeneration. *J. Energy Resour. Technol.* **2015**, *137*, No. 042002.

(2) Afkhamipour, M.; Mofarahi, M. Comparison of rate-based and equilibrium-stage models of a packed column for post-combustion CO2 capture using 2-amino-2-methyl-1-propanol (AMP) solution. *Int. J. Greenhouse Gas Control* **2013**, *15*, 186−199.

(3) Thee, H.; Nicholas, N. J.; Smith, K. H.; da Silva, G.; Kentish, S. E.; Stevens, G. W. A kinetic study of CO2 capture with potassium carbonate solutions promoted with various amino acids: Glycine, sarcosine and proline. *Int. J. Greenhouse Gas Control* **2014**, *20*, 212−222.

(4) Smith, K.; Lee, A.; Mumford, K.; Li, S.; Thanumurthy, N.; Temple, N.; Anderson, C.; Hooper, B.; Kentish, S.; Stevens, G.; Indrawan. Pilot plant results for a precipitating potassium carbonate solvent absorption process promoted with glycine for enhanced CO2 capture. *Fuel Process. Technol.* **2015**, *135*, 60−65.

(5) Isa, F.; Zabiri, H.; Ng, N. K. S.; Shariff, A. M. CO2 removal via promoted potassium carbonate: A review on modeling and simulation techniques. *Int. J. Greenhouse Gas Control* **2018**, *76*, 236−265.

(6) Mustafa, N. F. A.; Mohd Shariff, A.; Tay, W. H.; Abdul Halim, H. N.; Mhd Yusof, S. M. Mass Transfer Performance Study for CO2 Absorption into Non-Precipitated Potassium Carbonate Promoted with Glycine Using Packed Absorption Column. *Sustainability* **2020**, *12*, No. 3873.

(7) Borhani, T. N. G.; Azarpour, A.; Akbari, V.; Alwi, S. R. W.; Manan, Z. A. CO2 capture with potassium carbonate solutions: A state-of-the-art review. *Int. J. Greenhouse Gas Control* **2015**, *41*, 142−162.

(8) Grimekis, D.; Giannoulidis, S.; Manou, K.; Panopoulos, K. D.; Karellas, S. Experimental investigation of CO2 solubility and its absorption rate into promoted aqueous potassium carbonate solutions

at elevated temperatures. *Int. J. Greenhouse Gas Control* **2019**, *81*, 83−92.

(9) Ngu, L.; Mahmoud, A.; Sunarso, J. In Aspen Plus simulation-based parametric study of Benfield process using hot potassium carbonate promoted by diethanolamine. *IOP Conf. Ser.: Mater. Sci. Eng.* **2020**, *778*, No. 012058.

(10) Al-Naimi, S. A.; Jasim, F. T.; Kokaz, A. N. Dynamic Study of Carbon Dioxide Absorption Using Promoted Absorbent in Bubble Column Reactor. *J. Eng. Technol.* **2019**, *37*, 70−78.

(11) Bui, M.; Gunawan, I.; Verheyen, V.; Feron, P.; Meuleman, E.; Adeloju, S. Dynamic modelling and optimisation of flexible operation in post-combustion CO2 capture plants—A review. *Comput. Chem. Eng.* **2014**, *61*, 245−265.

(12) Chikukwa, A.; Enaasen, N.; Kvamsdal, H. M.; Hillestad, M. Dynamic modeling of post-combustion CO2 capture using amines—a review. *Energy Procedia* **2012**, *23*, 82−91.

(13) Harun, N.; Nittaya, T.; Douglas, P. L.; Croiset, E.; Ricardez-Sandoval, L. A. Dynamic simulation of MEA absorption process for CO2 capture from power plants. *Int. J. Greenhouse Gas Control* **2012**, *10*, 295−309.

(14) Grant, T.; Anderson, C.; Hooper, B. Comparative life cycle assessment of potassium carbonate and monoethanolamine solvents for CO2 capture from post combustion flue gases. *Int. J. Greenhouse Gas Control* **2014**, *28*, 35−44.

(15) Salvinder, K. M. S.; Zabiri, H.; Isa, F.; Taqvi, S. A.; Roslan, M. A. H.; Shariff, A. M. Dynamic modelling, simulation and basic control of CO2 absorption based on high pressure pilot plant for natural gas treatment. *Int. J. Greenhouse Gas Control* **2018**, *70*, 164−177.

(16) Salvinder, K. M. S.; Zabiri, H.; Taqvi, S. A.; Ramasamy, M.; Isa, F.; Rozali, N. E. M.; Suleman, H.; Maulud, A.; Shariff, A. M. An overview on control strategies for CO2 capture using absorption/stripping system. *Chem. Eng. Res. Des.* **2019**, *147*, 319−337.

(17) Sultan, T.; Zabiri, H.; Taqvi, S. A. A.; Shahbaz, M. Plant-wide MPC control scheme for CO2 absorption/stripping system. *Mater. Today: Proc.* **2021**, *42*, 191−200.

(18) Sultan, T.; Zabiri, H.; Shahbaz, M.; Maulud, A. S. Performance evaluation of the fast model predictive control scheme on a CO2 capture plant through absorption/stripping system. *Process Saf. Environ. Prot.* **2022**, *157*, 218−236.

(19) Hairul, N.; Shariff, A.; Bustam, M. Process behaviour in a packed absorption column for high pressure CO2 absorption from natural gas using PZ+ AMP blended solution. *Fuel Process. Technol.* **2017**, *157*, 20−28.

(20) Isa, F.; Zabiri, H.; Shaarif, M. A. CO2 removal via promoted potassium carbonate with glycine: solubility measurement at elevated pressure. *IOP Conf. Ser.: Mater. Sci. Eng.* **2019**, *702*, No. 012039.

(21) Shaikh, M. S.; Azmi, M. S.; Bustam, M. A.; Murshid, G. In Study of CO2 solubility in aqueous blend of potassium carbonate promoted with glycine. *Appl. Mech. Mater.* **2014**, *625*, 19−23.

(22) Shuaib, S. M.; Shariff, A. M.; Bustam, M. A.; Murshid, G. Physical properties of aqueous solutions of potassium carbonate+ glycine as a solvent for carbon dioxide removal. *J. Serb. Chem. Soc.* **2014**, *79*, 719−727.

(23) Dutta, R.; Nord, L. O.; Bolland, O. J. Applicability and validation of use of equilibrium-based absorber models with reduced stage efficiency for dynamic simulation of post-combustion CO2 capture processes. *Energy Procedia* **2017**, *114*, 1424−1433.

(24) Peng, J.; F Edgar, T.; Bruce Eldridge, R. Dynamic rate-based and equilibrium models for a packed reactive distillation column. *Chem. Eng. Sci.* **2003**, *58*, 2671−2680.

(25) Lee, A.; Mumford, K. A.; Wu, Y.; Nicholas, N.; Stevens, G. W. Understanding the vapour−liquid equilibrium of CO2 in mixed solutions of potassium carbonate and potassium glycinate. *Int. J. Greenhouse Gas Control* **2016**, *47*, 303−309.

(26) Lee, A.; Wolf, M.; Kromer, N.; Mumford, K. A.; Nicholas, N. J.; Kentish, S. E.; Stevens, G. W. A study of the vapour−liquid equilibrium of CO2 in mixed solutions of potassium carbonate and potassium glycinate. *Int. J. Greenhouse Gas Control* **2015**, *36*, 27−33.

(27) Jayakumar, K.; Panda, R. C.; Panday, A. A Review: State-of-the-Art LPG Sweetening Process. *Int. J. Greenhouse Gas Control* **2017**, *9*, 175−206.

(28) Kaur, H.; Chen, C. C. Thermodynamic modeling of CO2 absorption in aqueous potassium carbonate solution with electrolyte NRTL model. *Fluid Phase Equilib.* **2020**, *505*, No. 112339.

(29) Zhang, Y.; Chen, C.-C. Thermodynamic Modeling for CO2 Absorption in Aqueous MDEA Solution with Electrolyte NRTL Model. *Ind. Eng. Chem. Res* **2011**, *50*, 163−175.

(30) Hartono, A.; Ahmad, R.; Svendsen, H. F.; Knuutila, H. K. New solubility and heat of absorption data for CO2 in blends of 2-amino-2-methyl-1-propanol (AMP) and Piperazine (PZ) and a new eNRTL model representation. *Fluid Phase Equilib.* **2021**, *550*, No. 113235.

(31) Hartono, A.; Rafiq, A.; Gondal, S.; Svendsen, H. F. Solubility data for Nitrous Oxide (N2O) and Carbon dioxide (CO2) in Piperazine (PZ) and a new eNRTL model. *Fluid Phase Equilib.* **2021**, *538*, No. 112992.

(32) Akinola, T. E.; Oko, E.; Wang, M. Study of CO2 removal in natural gas process using mixture of ionic liquid and MEA through process simulation. *Fuel* **2019**, *236*, 135−146.

(33) Kuramochi, H.; Noritomi, H.; Hoshino, D.; Nagahama, K. Measurements of vapor pressures of aqueous amino acid solutions and determination of activity coefficients of amino acids. *J. Chem. Eng.* **1997**, *42*, 470−474.

(34) Mondal, B. K.; Bandyopadhyay, S. S.; Samanta, A. N. VLE of CO2 in aqueous sodium glycinate solution−New data and modeling using Kent−Eisenberg model. *Int. J. Greenhouse Gas Control* **2015**, *36*, 153−160.

(35) Liu, J.; Wong, D. S.-H.; Chen, D.-S. Energy-saving performance of advanced stripper configurations for CO2 capture by ammonia-based solvents. *J. Taiwan Inst. Chem. Eng.* **2020**, *113*, 273−284.

(36) Smith, K.; Xiao, G.; Mumford, K.; Gouw, J.; Indrawan, I.; Thanumurthy, N.; Quyn, D.; Cuthbertson, R.; Rayer, A.; Nicholas, N.; Lee, A.; da Silva, G.; Kentish, S.; Harkin, T.; Qader, A.; Anderson, C.; Hooper, B.; Stevens, G. Demonstration of a Concentrated Potassium Carbonate Process for CO2 Capture. *Energy Fuels* **2014**, *28*, 299−306.

(37) Zhang, S.; Ye, X.; Lu, Y. Development of a Potassium Carbonate-Based Absorption Process with Crystallization-Enabled High-Pressure Stripping for CO2 Capture: Vapor−Liquid Equilibrium Behavior and CO2 Stripping Performance of Carbonate/Bicarbonate Aqueous Systems. *Energy Procedia* **2014**, *63*, 665−675.

(38) Ochieng, R.; Berrouk, A.; Peters, C.; Slagle, J.; Lyddon, L.; Krouskop, P. Simulation of the Benfield HiPure process of natural gas sweetening for LNG production and evaluation of alternatives *Proceedings of Sour Oil Gas Advanced Technology* 2012.

(39) Hairul, N.; Shariff, A.; Bustam, M. Mass transfer performance of 2-amino-2-methyl-1-propanol and piperazine promoted 2-amino-2-methyl-1-propanol blended solvent in high pressure CO2 absorption. *Int. J. Greenhouse Gas Control* **2016**, *49*, 121−127.

(40) Smith, K. H.; Harkin, T.; Mumford, K.; Kentish, S.; Qader, A.; Anderson, C.; Hooper, B.; Stevens, G. W. Outcomes from pilot plant trials of precipitating potassium carbonate solvent absorption for CO2 capture from a brown coal fired power station in Australia. *Fuel Process. Technol.* **2017**, *155*, 252−260.

(41) Yi, F.; Zou, H.-K.; Chu, G.-W.; Shao, L.; Chen, J.-F. Modeling and experimental studies on absorption of CO2 by Benfield solution in rotating packed bed. *Chem. Eng. J.* **2009**, *145*, 377−384.

(42) Yadav, E. S.; Indiran, T. PRBS based model identification and GPC PID control design for MIMO Process. *Mater. Today: Proc.* **2019**, *17*, 16−25.

(43) Bedelbayev, A.; Greer, T.; Lie, B. In *Model Based Control of Absorption Tower for CO2 Capturing*, 49th Scandinavian Conference; Citeseer, 2008, pp 7−8.

(44) Panahi, M.; Skogestad, S. Economically efficient operation of CO2 capturing process. Part II. Design of control layer. *Chem. Eng. Process* **2012**, *52*, 112−124.

(45) Zhang, Q.; Turton, R.; Bhattacharyya, D. Development of model and model-predictive control of an MEA-based postcombustion CO2 capture process. *Ind. Eng. Chem. Res.* **2016**, *55*, 1292−1308.